Excilamps and their applications

M.I. Lomaev[1,2]*, E.A. Sosnin[1,2], V.F. Tarasenko[1,2]
[1]Institute of High Current Electronics, Akademicheskii Ave. 2/3, 634055 Tomsk, Russia
[2]National Research Tomsk State University, Lenina Ave. 36, 634050 Tomsk, Russia

*Correspondence: M.I. Lomaev (E-mail: Lomaev@loi.hcei.tsc.ru), National Research Tomsk State University, Lenina Ave. 36, 634050 Tomsk, Russia

Abstract

The paper covers the description of a new class of sources of spontaneous ultraviolet and vacuum ultraviolet radiation – excilamps, based on the nonequilibrum radiation of exciplex or excimer molecules. The design and some technical characteristics of traditional excilamps excited by a dielectric barrier discharge are presented. The data concerned new types excilamps excited by runaway electrons preionized diffuse discharge both in single and pulse-periodic modes are given, as well. Some new applications of excilamps in photochemistry, effect of ultraviolet and vacuum ultraviolet radiation on the physiological action of living organism, photosynthesis and growth of plants, and use of excilamps for pre-sowing treatment of seeds are described.
Keywords: Excilamp, Gas-phase VUV photochemistry, Runaway electrons preionized diffuse discharge

1. Introduction

Excilamps are a general name of devices that emit spontaneous nonequilibrum ultraviolet (UV) and/or vacuum ultraviolet (VUV) radiation of excimer and exciplex molecules. Now, a great variety of excilamps is available. ((Table 1)) The devices are classified by the type of working molecules (Tab. 1), gas excitation method, and design [1]. The year of 2015 marks the anniversary since the beginning of excilamp research at the Institute of High Current Electronics (IHCE) RAS (Tomsk, Russia). During this period, 18 excilamps and photochemical reactors have been designed and their wide applicability has been proven. The present review covers our experience in designing excilamps, including new ones, excited by runaway electrons preionized diffuse discharge, and their use in photochemistry and other applications. Research data obtained by our colleagues can be found elsewhere [2-10].

2. Dielectric Barrier Discharge Driven Excilamps

Dielectric barrier discharge excilamps or abbreviated DBD-driven excilamps are the most popular type of lamps, which find various practical applications. The dielectric barrier discharge (DBD) is a discharge between electrodes in which the conductivity current is limited by at least one dielectric layer. Closing of a circuit, including a dielectric barrier, requires an ac or pulsed voltage generator. The discharge ignited in the interelectrode gap under these conditions has a specific form and normally consists of numerous microdischarges with discharge current densities of 0.1–1 kA·cm^{-2} and

Received: April 21, 2015; revised: July 20, 2015; accepted: July 28, 2015

To be cited as: Chem. Eng. Technol. 10.1002/ceat.201500229

Link to final VoR: http://dx.doi.org/10.1002/ceat.201500229

electron density of up to 10^{12}–10^{15} cm^{-3} at an electric field strength of 0.1–100 $kV{\cdot}cm^{-1}$. Microdischarges represent zones of increased current density shaped as a cylinder or two cones with facing vertices and bases on the dielectric surface. Their form, density (number per unit surface), and brightness of their glow depend on a gas mixture and pressure, gas gap width, excitation power, and pulse repetition frequency. The dielectric serves as an energy limiter in a microdischarge and provides uniform distribution of microdischarges over the entire surface of the dielectric-coated electrode. The presence of dielectric barriers to the current flow results in electric charge accumulation on their surfaces where the electric field opposes the external electric field such that the current cuts off with energy release into the current transport regions. At the same time, due to the applied external voltage, the electric field in rest of the gap free of electric current and surface charges remains high. This provides a rather uniform distribution of the current and excitation power in the discharge volume at increased gas pressures.

The DBD plasma is highly nonequilibrium. The characteristic temperature of heavy particles is comparable to the temperature of dielectric barriers and is normally no greater than 100 °C. This property of barrier discharges is widely used in many industrial technologies, which are based on nonequilibrium low-temperature plasmas (ozone production, surface treatment and material modification, manufacture of plasma panels, industrial waste utilization, etc) [1-10]. A remarkable property by which dielectric barrier discharges are distinguished from other types of discharge is the possibility to control the average electron energy and density in a wide range of external parameters such as the discharge gap geometry and dielectric type. Moreover, the initiation of a barrier discharge in a sealed-off chamber made of dielectric material (quartz, glass, ceramics) with the electrodes placed on the outside allows one to attain both spectral purity and long lifetime of the working mixture [1]. ((Figure 1)) Fig. 1 presents different designs of DBD-driven excilamps used by now.

In terms of applicability, the advantages of DBD-driven excilamps can be outlined as follows. 1) The radiation of excilamps is narrow-band and its halfwidth is 2–15 nm for exciplex molecules RgX^* and 2–30 nm for excimers of rare gases Rg_2^*, which provides their wide use in selective photochemistry (Rg – rare gas atom, X – halogen's atom). 2) The specific radiant flux ($W{\cdot}cm^{-3}$) of excilamps is higher than that of typical low-pressure mercury lamps. 3) Their designs can follow a variety of concepts (Fig. 1). 4) The discharge ignition in excilamps is easy and their maximum power after switching is attained in less than 1 s for which no special control gear are normally required. 5) Their operation features comparative electrical safety. 6) The useful life of the best excilamps or the time t^k during which the radiation flux of an excilamp decreases by k percent is $t^{15–20}$ > 10000 h for chlorine-containing excilamps and t^5 > 10000 h for those filled with rare gases; this parameter is often decisive for practical application of light sources. Finally the bulbs of excilamps contain no mercury, except for those on mercury halogenides HgX^*, which is urgent in view of EU directive 2011/65/EU on hazardous substances.

We have developed several models of excilamps and photoreactors based on a DBD-driven excilamp. The devices are rather cheap (an excilamp is priced at least 10 times less than a UV or VUV laser) and their applicability has been proven almost in all known photoprocesses requiring UV and/or VUV radiation. Therefore, in many applications where narrow-band irradiation of extended objects is required to meet up-to-date ecological standards and radiation coherence is irrelevant, excilamps are a good alternative to lasers. In terms of the cost per watt of radiation, excilamps against UV light emission diodes operating at a wavelength of 200–300 nm are also beyond comparison.

Below we give examples of our DBD-driven excilamp and photoreactor designs.

((Figure 2)) ((Table 2)) Series BD_P (barrier discharge, portable), Fig. 2a). An excilamp of this series is a portable coaxial excilamp placed in a housing with air-cooling and reflector. The excilamp is rather small in dimensions and weight and is convenient for scientific research. An experimental arrangement with a BD_P excilamp for irradiation of rather small liquid volumes in laboratory conditions is presented in Fig. 2c). The use of photoreactor of this type is reported, for example, elsewhere [11].

Series BD_EL (barrier discharge, extra large), Fig. 2b). An excilamp of this type is a long coaxial excilamp placed in a housing with air-cooling and reflector. This model is basic for excilamps on working molecules $KrCl^*$, $XeCl^*$, and $XeBr^*$. The flange for output radiation is shaped to dimensions of 85×10 cm. The excilamp is convenient for irradiation of large surfaces or volumes with an optically transparent medium (gases, liquids).

((Table3)) Series BD_R (barrier discharge, reactor). An excilamp of this series is intended for intense irradiation of solutions and gases and represents the so-called flow photoreactor [12] in which an irradiated medium is passed through a quartz tube in the internal excilamp cavity. A general view of the excilamps models and their parameters are presented in
Fig. 2c), Fig. 2d) and Tab. 3, respectively.

These and other models of DBD-driven excilamps were used to advantage by different research groups in photochemical studies of aqueous solutions of organic substances [13-16] and in research in photochemical control of biological processes [17].

3. Short pulse excilamps pumped by a runaway electrons preionized diffuse discharge

DBD-driven excilamps, described above, operate in pulse-periodic mode at pulse repetition rate of tens – hundreds kHz and have a lifetime of up to 10000 h, enough for many practical applications. The typical values of an average and pulse radiation power density do not exceed 100 $mW{\cdot}cm^{-2}$ and tens $W{\cdot}cm^{-2}$, respectively. Nevertheless, some applications require radiation sources with higher specific output parameters as compare to above-mentioned ones. The possible way to create a high power UV/VUV pulsed light sources – use of high-pressure diffuse discharges formed without preionization of discharge gap with external ionization sources. Despite the disadvantage - a small resource, light sources based on these discharges allow to obtain a radiation power density up to 1 $MW{\cdot}cm^{-3}$.

Currently the discharges formed in various gases without preionization of discharge gap with external ionization sources attract much attention [18]. The peculiarities of runaway electrons preionized diffuse discharge (REP DD) excitation – high overvoltages, high specific excitation powers, and possibility of REP DD at increased gas pressures – predetermine in many respects the radiative properties and main plasma parameters of this type of discharge. The short duration and high specific powers of excitation at increased gas pressures result in dense low-temperature plasma in which most of the energy deposited in the medium is stored in internal degrees of freedom – as ionization and excitation energy of atoms or gas molecules. In its volume form, the REP DD operating under high thermodynamic nonequilibrium conditions produces intense luminescence both at the stage of energy deposition and at the stage of plasma recombination. At the same time, some practical applications require spontaneous and induced radiation sources with high pulse power in the UV and VUV spectral regions.

Now, the most commonly used media in producing high-power narrowband UV and VUV radiation are heavy rare gases and their mixtures with halogens [19]. Excitation of these gases and their mixtures by diffuse discharge at increased pressure provides efficient formation of excimer or exciplex molecules. First, these molecules feature the presence or absence of strong chemical bond in electron-excited and ground states, resulting in broad emission bands on their radiative decay. Second, the formation of electron-excited states is a consequence of plasma chemical reactions occurring on excitation of the gases. The relaxation from highly excited and ionized states to lower excited states is thus radiationless due to numerous intersections of their potential energy curves. The further transition of a molecule from lower excited states to the ground state can be only radiative with subsequent decay of the molecule. This predetermines the possibility to obtain highly efficient radiation and radiation spectrum dominated by bands of excimers (exciplexes). The lifetime of such molecules in the excited state can span from 10^{-9} to 10^{-7} s. Their spontaneous decay into separate atoms involves release of a photon of energy 2.5–10 eV characteristic of a given molecule.

The elevated pressure and high specific excitation power limit the choice of optical media and determine the peculiarities of their kinetics in high-power pulsed gas discharge sources of spontaneous radiation. Therefore, for example, under these conditions it is impossible to use radiation at resonance transitions due to discharge plasma self-absorption. At the same time, dimers of rare gases efficiently form in three-body collisions of atoms at high pressures. It is well known that as the pressure is increased, the radiation spectrum of dimers of rare gases is dominated by the so-called second continuum [20, 21]. Besides, increasing the gas pressures decreases the radiation pulse width and can change the halfwidth and number of bands in the radiation spectrum. Increasing of the specific excitation power increases the degree of plasma excitation and ionization, which, as a rule, leads to a decrease in the formation efficiency of working molecules. For excimer molecules, the efficiency decreases due to increasing temperature and quenching of the working particles in collisions with electrons. For exciplex molecules, the increase in excitation power changes the main channel of their formation: from harpoon reaction to ion-ion recombination.

3.1. Amplitude-time and spectral characteristics of radiation in REP DD.

The amplitude-time and spectral characteristics of plasma radiation in one or another type of discharge are the most important parameters of discharge-based spontaneous radiation sources. Of particular significance for high-power pulsed sources are the specific radiation power, and the size and luminosity distribution of a glowing plasma volume. The plasma of constricted pulsed discharges, as a rule, provides higher specific radiation power and broader emission bands compared to the plasma of pulsed volume discharges formed with external ionization and to the plasma of barrier discharges. The exception is the REP DD plasma in which the attained narrowband radiation power density is ~1 MW·cm^{-3} at a xenon pressure of ~12 atm [22], which is commensurable with the radiation power density in the plasma of a constricted pulsed discharge.

Although different types of discharges differ in their peculiar radiative features, they also have common characteristics - spectral composition and dependence on gas or gas mixture pressure. To obtain maximum output parameters of a radiation source, the gas pressure is normally as high as possible.

Nanosecond pulsed volume discharges in an inhomogeneous electric field with a high specific power of up to 800 MW·cm^{-3} and specific energy deposition of ~1 J·cm^{-3} are quite promising for generating high-power pulsed radiation fluxes in controllable and rather easily reproducible conditions. To do this, it is most appropriate to use working media in which radiating particles form during plasma decay stage. Among these media are rare gases and their mixtures with halogens [19, 23]. The radiation pulse width can thus be tens and hundreds of nanoseconds. The short excitation pulse width of about several nanoseconds also provides a possibility to obtain short high-power radiation pulses in those working media in which radiation takes place predominantly during the excitation stage, for example, in nitrogen.

3.2. Excilamps on rare gas dimers.

((Figure 3)) It is known that heavy rare gases display high luminous efficacy both on excitation by constricted discharges and on their excitation by volume discharges. Therefore, most of the research in the radiative characteristics of REP DD plasma was conducted with these gases. A block diagram of the experimental setup used in studies of the discharge formation and in measurements of the amplitude-time and spectral characteristics of radiation in the range from 120 to 850 nm is shown in Fig. 3.

((Figure 4)) The voltage pulses applied to a discharge gap were produced by the RADAN-220 generator. The wave impedance of the generator was 20 Ohm. In the idle mode, the voltage pulse produced by the generator in the discharge gap had an amplitude of ~250 kV and full width at half maximum (FWHM) of ~2 ns with a matched load at a voltage pulse rise time of ~0.5 ns. The gas diode design is shown in Fig. 4a). The inner diameter of the gas chamber was 48 mm. The electrodes were a plane anode and a cathode of small curvature radius, which ensured field amplification near the cathode. The cathode was a tube made of steel foil of diameter ~6 mm and thickness 50 μm. The tube was fixed on a metal rod of the same diameter. The plane anode was a brass plate connected to the chamber case via a shunt composed of heat- and moisture-resistant bulk resistors or small-sized chip resistors. The interelectrode gap was varied from 4 to 16 mm.

The gases were excited by a REP DD and also by a constricted discharge which was realized due to the use of a shorter discharge gap and pointed steel cathode. Signals from the current shunt were recorded by a TDS-3034 oscilloscope (0.3 GHz, 2.5 $Gs \cdot s^{-1}$). Images of the discharge glow were taken with a digital camera. Radiation spectra were registered with an EPP2000C-25 spectrometer (StellarNet-Inc.) with known spectral sensitivity in the range from 200 to 850 nm and with a VM-502 vacuum monochromator (Acton Researcher Corp.) in the range from 120 to 540 nm. To obtain spectra in the range from 120 to 850 nm, the spectra registered by these devices for wavelengths in the vicinity of 200 nm were joined. The time behavior of radiation intensity in individual spectral ranges were determined using an EMI 9781 B photomultiplier tube, which ensured recording of radiation pulses with a risetime of up to ~3 ns and decay time of up to ~30 ns, and also a FEK-22SPU photodiode with a time resolution of ~1 ns. The radiation energy was measured using a calibrated photodetector (Ophir Optronics Inc) with a PE50BB photodetector head. To eliminate the influence of absorption by air, the photodetector head was located in the pumped volume at a distance of 10 cm from the longitudinal axis of the discharge gap. The portion of radiation incident on the photodetector at characteristic plasma formation sizes of ~1 cm was calculated using the point source model.

With no external preionization, volume discharges were obtained in xenon, krypton, and argon at a pressure of 0.3–1.2 atm. A photo of the discharge glow in xenon at a pressure of 1.2 atm is shown in Fig. 4b) [24]. It is seen that the discharge is formed as a set of diffuse jets distributed over the external boundary of a truncated cone. On the electrodes, primarily on the cathode, bright spots of size no larger than ~1 mm are observed. During the formation of the REP DD, no current spike of opposite polarity was present on the oscillogram of the discharge current, being indicative of total energy transfer from the generator to the discharge plasma. The energy deposited in the discharge plasma in xenon at a pressure of 1.2 atm was ~1 J by estimation from the energy stored in the high-voltage line of the generator and from the short-circuit current. The specific excitation power under these conditions was no less than 100 $MW \cdot cm^{-3}$.

((Figure 5)) In all heavy rare gases, high-power broadband radiation at the $B^1\Sigma^+_u \rightarrow X^1\Sigma^+_g$, $A^3\Sigma^+_u \rightarrow X^1\Sigma^+_g$ transitions of dimers in the VUV region was detected (Fig. 5). The spectral halfwidth of bands for xenon, krypton, and argon at a pressure of 1.2 atm was ~18, ~13, and ~8 nm, respectively. The radiation energy of xenon, krypton, and argon dimers was no less than 90 % of the total radiation energy in the range from 120 to 850 nm. The broadband radiation in the UV and visible spectral regions was much less intense. The highest broadband radiation intensity of dimers was observed in xenon. In krypton and argon, the radiation intensity was respectively ~1.5 and ~2 times lower (the spectra in Fig. 5 are presented with regard to relative spectral sensitivity at λ = 126, 146, and 172 nm).

To determine the influence of the excitation mode and discharge operation mode on the spectral characteristics of radiation, the radiation spectra in xenon were measured at different pressures (from 0.3 to 1.2 atm) and different interelectrode gaps (from 4 to 16 mm). The radiation energy measured by the Ophir calorimeter was ~40 mJ to a full solid angle and the radiation power was ~500 kW. This type of sources can be used, for example, for XeF_2 dissociation in the active medium of an optically pumped XeF laser on C–A transition [25]. Note that the above values of the radiation energy and power are not the limit for this setup. The measurements give slightly underestimated values of the radiation energy and power of xenon dimers because part of the excitation energy is lost in a shunting discharge from the cathode holder to the case.

((Figure 6)) As the pressure was increased to 12 atm, the most homogeneous discharge was obtained in helium. A supershort avalanche electron beam in helium at this pressure was detected for the first time. The FWHM of the beam current pulse was no more than 100 ps. At the same time in xenon, constriction channels are observed even at a pressure of 3–4 atm. Nevertheless, at a pressure of 12 atm, high-power radiation of the xenon dimer band is also detected (Fig. 6). The main feature of the radiation spectrum in the discharge at high pressure (up to 15 atm) is the presence of continuum in the UV and visible spectral regions. The continuum is mainly due to recombination transitions [26]. Lines of the transitions XeI, XeII, and XeIII are present in the UV and visible spectral regions.

Dependences of the FWHM, maximum power of VUV radiation on the xenon pressure are presented in Fig. 6. It is seen that the radiation power increases with increasing the xenon pressure. The maximum power ~ 1 MW/cm^3 and the shortest radiation pulse width ~ 8 ns were obtained at a pressure of 12 atm. The decrease in pulse width and the increase in radiation power with increasing xenon pressure owe to faster formation of xenon dimers Xe_2^* in association reaction (1) and to their faster radiationless quenching by xenon atoms Xe (2):

$$Xe^* + Xe + Xe \rightarrow Xe_2^* + Xe \quad (1)$$

$$Xe_2^* + Xe \rightarrow Xe + Xe + Xe \quad (2)$$

Estimates show that the increase in pressure from 1 to 12 atm increases the probability of Xe^* entering into reaction (2) from ~ $3.3\cdot10^7$ s^{-1} to ~ $5\cdot10^9$ s^{-1}.

The REP DD holds promise for creation of lasers on rare gas dimers. Calculation of the plasma afterglow characteristics in nanosecond discharges in Xe [27] and Kr [28] show that at a pressure of 5–10 atm, the gain can amount to ~ 0.05–0.1 cm^{-1} that is sufficient for generation. It should be noted that excitation by short pulses provides an optimum mode of plasma lasing with self-sustained discharge pumping [23]. The excitation pulse width is several nanoseconds and the generation is bound to occur during the afterglow when the absorption of the active medium at the laser wavelength becomes lower.

((Figure 7)) Of great significance for the prospects of obtaining induced VUV radiation are the results of studies on REP DD excitation of binary argon and krypton mixtures with small (~0.01 %) xenon additives [29]. The studies show that in addition to radiation of argon and krypton dimers, narrowband radiation at λ ~ 147 nm with a FWHM of ~ 1 nm is detected (Fig. 7). The radiation in this region, according to [30], is due to bands of heteronuclear ArXe* and KrXe* dimers. The spectral power density of ArXe* and KrXe* molecules at λ ~ 147 nm is respectively higher than and comparable (at no more than 0.6 atm) to the spectral power density of argon and krypton dimers. The intensity of this band in argon was highest at a pressure of 0.9 atm (Fig. 7) and in krypton at a pressure of 0.3 atm. The time dependence of radiation at ~147 nm roughly corresponded to that of argon and krypton dimers. The results are indicative of the possibility to obtain VUV radiation of ArXe* and KrXe* molecules at λ ~ 147 nm.

3.3. Excilamps on rare gas halogenides.

The radiative characteristics of REP DD-excited mixtures of rare gases with halogens were studied on the working media much used in the UV spectral region: Xe–Cl_2, Kr–Cl_2, Xe–Br_2, and Kr–Br_2 [31]. In the experiments, the discharge chamber same shown in Fig. 4a) was used. The inner diameter of the chamber was 36 mm. The discharge was ignited between a plane anode and a tubular steel cathode. The high-voltage pulses applied to the cathode from a RADAN-150 generator had a rise time of ~1 ns and amplitude of ~150 kV (voltage in the idle mode).

((Figure 8)) Optimization of the binary mixtures in pressure and rare gas to halogen ratio revealed the following. At low pressures (60–120 Torr) and interelectrode gap of 12 mm, the discharge represented a homogeneous diffuse glow of conical shape. As the pressure was increased, the discharge assumed the form of a diffuse channel of diameter ~3 mm that was transformed to a spark at a pressure above 500 Torr. As the halogen content in the working mixture was increased, the discharge was constricted at lower pressures and the radiation power decreased. The maximum radiation power densities in volume discharges in Xe–Cl_2, Kr–Cl_2, and Xe–Br_2 were obtained at a pressure of ~500 Torr and rare gas/halogen ratio of 50/1. For Kr–Br_2, the optimum pressure and mixture ratio for attaining the maximum radiation power density was 750 Torr and Kr/Br_2=100/1, respectively. The maximum radiation power densities of $KrCl^*$, $XeCl^*$, $XeBr^*$, and $KrBr^*$ molecules were 3.7, 3, 4.5, and 2 $kW{\cdot}cm^{-2}$ (Fig. 8) at an efficiency of 5, 4.8, 5.5, and 4 %, respectively. Under these conditions, the energy deposited in the discharge plasma was 1 *J*.

((Figure 9)) The voltage across the discharge gap, discharge current, and time dependence of the radiation pulse of a $XeBr^*$ molecule at a pressure of 500 Torr are shown in Fig. 9. The FWHM of radiation pulses in the volume discharges in the halogenides of rare gases with optimum light yields was 30–40 ns.

The radiation spectra of the plasma glow in nanosecond volume discharges in Kr–Cl_2, Xe–Cl_2, and Xe–Br_2 consisted of rather narrow (few nanometers at half maximum) bands of intense B–X transitions and weak D–A and C–A transitions corresponding to exciplex molecules and were similar to the radiation spectra of barrier discharge-driven excilamps [1]. As the pressure of the working mixture was increased, the energy in the bands of D–A and C–A transitions decreased, and at pressure of 500 Torr, up to 90 % of the total radiation energy was concentrated in the B–X bands. The radiation spectrum of the discharge glow in Kr–Br_2 consisted of B–X bands of $KrBr^*$ (206 nm) and Br^*_2 (289 nm), and also C–A bands (222 nm) and B–A bands (228 nm) of $KrBr^*$. The intensities of the bands of $KrBr^*$ and Br^*_2 molecules varied depending on the Br_2 content in the working mixture: the larger the fraction of Br_2, the less intense are the B–X, C–A, and B–A bands of $KrBr^*$.

((Figure 10)) Rather intense luminescence in the UV region can be obtained at certain transitions of other gases, in particular nitrogen. In the REP DD plasma, the above values of *E/p* are easy to attain and this provides a possibility to obtain intense luminescence at the transitions of the second positive (2^+) nitrogen system [32]. Typical emission spectrum of plasma of REP DD in atmospheric-pressure nitrogen is shown in Fig. 10.

4. Point-like pulse-periodic UV radiation source with a short pulse duration

The metal vapor at pulse-periodic mode of REP DD was shown experimentally to penetrate in a gas gap. On this basis, point sources of spontaneous radiation can be created [33]. They operate in atmospheric-pressure air and emit on optical transitions of electrode materials atoms. In [33] the FPG-10 generator with a voltage pulse amplitude up to 12.5 kV in the transmission line was used. The generator was connected to the discharge gap via a 50-Ohm cable of length 1.3 m. The discharge was formed in the atmospheric pressure air between the two electrodes terminating in cusps with small radii of curvature. They were made of stainless steel, aluminum, copper, titanium, tantalum, and tungsten. Stainless steel electrodes were standard medical needles with an outer diameter of 0.5 mm and the other electrodes were made of foils of these materials. The investigations were carried out with gaps of 0.5, 1, and 2 mm and a pulse repetition rate ranging from 370 to 1050 Hz. The experiments yielded the following results. A diffuse discharged was produced for an interelectrode gap of 2 mm, which turned into a spark gap when the interelectrode gap was made narrower, the diffuse discharge phase always being present early in the discharge formation in this case. This is clearly seen from the discharge photographs taken at different point in time with a CCD camera. The diffuse discharge phase supposedly corresponds to the REP DD. The half-amplitude radiation pulse duration was equal to ~3 ns for a gap of 2 mm (REP DD) and to about 70 ns for a gap of 0.5 mm (spark after REP DD). Such a long pulse duration in the case of a 0.5-mm gap is attributable the spectra contains the lines of neutral atoms and atomic ions of iron.

In the course of experiments, it was established that weak X-ray radiation emanated from the discharge gap. It was recorded using a scintillation detector as well as from an imprint on a photographic film opposite the window covered with a beryllium filter. The generation of X-ray radiation in the discharge gap is attributable of runaway electrons, which are generated at the initial stage of discharge formation and furnish the conditions for the REP DD.

The emission spectra for interelectrode gaps of 2, 1, and 0.5 mm were registered as well. For a 2-mm gap, the emission spectrum of REP DD was observed, primarily the bands of the (2^+) nitrogen system (Fig. 11a)). The spectrum at decreasing of the interelectrode gap from 2 mm to 0.5 mm was registered to change. In this case, it includes emission of the (2^+) nitrogen system bands, broadband continuum and additional spectral lines (Fig. 11b)). At that, the radiation power of the (2^+) nitrogen system decreased, while the broadband continuum and metal lines radiation powers became substantially higher. The majority of lines in the spark spectrum belong to the iron spectrum. The energy of radiation in the 200 – 300 nm spectral range accounted for ~40 % of the energy of radiation in the entire spectral range investigated (200 – 850 nm). For an interelectrode gap d = 1 mm, a smaller amount of energy was concentrated in the continuum and the iron spectral lines in comparison with the case of d = 0.5 mm. With the use of electrodes made of other materials (aluminium, copper, titanium, tantalum, and tungsten) the spectra contain the lines of neutral atoms and ions of these materials.

5. Application of excilamps

The properties of excilamps allow their use as UV and VUV light emitters in direct photolysis, advanced oxidation processes, surface modification, luminescent conversion of UV/VUV radiation to visible light, etc. These applications are described elsewhere [2-10]. At the same time, the devices can be applied to solve comparatively new classes of problems. Below we briefly dwell on our experience of these new applications as the ones, which hold great potential promise.

5.1. High-pressure gas-phase VUV photochemistry

((Table 4)) There are systems in which a water content is small. A system like this is natural gas extracted from wells with a small water percentage. If the gas is not dried out, gas condensate locks form in pipelines during its transport. In 2003, it was proposed to dry unstrapped gas with Xe_2 and KrCl excilamps [34]. The results of irradiation of natural gas with these lamps are presented in Tab. 4.

It is seen from the Tab. 4 that the greatest changes are found in C_3-C_6 and H_2O compounds. This is particular noticeable for the Xe_2 excilamp with which the water vapor concentration decreases from 0.25 to 0.15 mass % (1.67 times). Thus, the basic process is dimerization of hydrocarbons, as is normally the case in mixtures of water vapors with hydrocarbons. Early in the irradiation, this process is ensured by VUV photolysis and the radiation energy of the Xe_2 excilamp is expended in water homolysis [5, 36]:

$$H_2O + hv \rightarrow H_2O^* \rightarrow H + OH \qquad (3)$$

Further dimerization occurs in the reactions with hydroxyl radicals:

$$C_nH_{2n+2} + OH \rightarrow C_nH_{2n+1} + H_2O \qquad (4)$$

$$C_nH_{2n+1} + C_mH_{2m+1} \rightarrow C_{(n+m)}H_{2(n+m+1)} \qquad (5)$$

The observed increase in C_{6+} concentration (in gas condensate yield) and the decrease in water vapor concentration in natural gas were found interesting for use in gas industry and this was a spur to development of high-power photochemical reactors based on DBD-driven Xe_2 excilamps [37]. Note that especially for this purpose, Xe_2 excilamps with a radiation power density of 19–25 mW·cm^{-2} were designed to hold an external pressure of up to 60 atm. In 2006–2007, the photoreactors were successfully tested both in the pilot mode and directly at the site of the Myldzhinsky gas-condensate field and the irradiation method was patented [38].

((Figure 12)) The designed reactor was cascaded (Fig. 12). It was passed through full-scale tests directly at the Myldzhinsky gas-condensate field. Chromatograms of nonirradiated and irradiated gas condensates at a pressure gradient demonstrated that the increase in condensate yield on irradiation involved an increase in C_4 and C_5 hydrocarbon concentrations and a decrease in C_6 hydrocarbon concentration. Thus, retrograde condensation with liquid phase precipitation took place in the multicomponent gas system near its critical point with an isothermal decrease in pressure. Moreover, the use of the Xe_2 excilamp under rigorous operating conditions increased the gas condensate yield in the extracted gas by a factor of 2–3.

This type of devices can lay the groundwork for high-pressure gas-phase VUV photochemistry as a new scientific field.

5.2. Physiological action of radiation on living organisms

The physiological action of radiation emitted by XeCl excilamps on the human organism consists in absorption of soft ultraviolet by the skin (epidermis and dermis) with activation of different photochemical processes the most known of which is photosynthesis of group D vitamins. So in 1980, a spectrum of UV action on psoriasis was obtained showing that the wavelength of UV radiation for treatment of psoriasis patients is 296–313 nm [39]. The progress in excilamp research made possible reliable XeCl excilamps and successful treatment of other skin diseases such as vitiligo, eczema, and atopic dermatitis, which is reported in numerous papers. For example, the first successful attempt at treatment of fungus diseases was made in 2004 [40] and treatment of alopecia areata was realized to advantage in 2013 [41].

In 2012, E.A. Sosnin proposed to extend the research in the physiological action of radiation produced by a XeCl excilamp to animals. The reasoning behind the study was that animals in stockbreeding complexes are kept indoors throughout their life and this, while preventing the spread of epidemic diseases, deprive the animals of sunlight, including solar UV radiation of short wavelength (about 290–320 nm), which stimulates the physiological activity of animals in natural conditions via complex photochemical and physiological reactions. In particular, the latter processes increase the immunity and productivity of animals. Because the radiation spectrum of a XeCl excilamp corresponds to this physiologically active range of solar radiation, it was reasonable to pursue the study.

First, the physiological action of radiation was studied on outbred white mice to investigate its effect on the motion activity and activity of smooth muscles of intestines. On the 30th day after completion of the experiment, anatomical examination was conducted. The study did not reveal any toxic, embryotoxic, skin irritative, and allergic action of the radiation. The live mass was physiologically increased by 2.6–3.1 %; enhancement and improvement was found in the motion activity, respiratory function, and gastric peristalsis; the radiation was shown to predispose to multiple pregnancy of the animals [42].

In 2012–2013, in collaboration with Tomsk Agricultural Institute and Siberian Agrarian Group, the physiological action of a DBD-driven XeCl excilamp on sows was studied. It was shown that small irradiation doses decreased the death rate of newborn piglets more than two times.

((Figure 13)) The operating conditions of devices in stockbreeding complexes are "aggressive"; the air is saturated with dust and biological gases. This makes impossible long-term operation of conventional air-cooled excilamps like those shown in Fig. 2. Therefore, specially to solve this problem, a protected XeCl excilamp operating with no cooling but ensuring the desired irradiation doses was developed (Fig. 13).

The results obtained require not only practical implementation but also reconsiderations based on photochemical and photophysical research. However, it is clear even now, that DBD-driven XeCl excilamps give hope for their wide application in the future, in particular to assist technological processes in animal breeding [43].

5.3. Photoregulation of agricultural plants

The potential of excilamps is still far from being unveiled in full. This is evidenced by research in photoregulation of plants by UV radiation. Radiation sources can provide efficient control of photosynthesis and growth of plants. One of the ways of increasing the photosynthetic activity of plants is to use a light source emitting at λ ~ 300–800 nm and ideally, such that its radiation is concentrated at 400–510 and 610–720 nm. Another way is to use UV radiation. In plants, this radiation changes the activity of enzymes and hormones and affects the synthesis of pigments as well as the rates of photosynthesis and photoperiodic reaction [44]. Our earlier laboratory research in the effect of UV radiation on photocontrol of plants suggested the following [45]:

1) Broadband irradiation simulative of solar radiation fails to provide exact information on how the growth of plants is disturbed;

2) Besides hazardous effects, UV radiation is likely to produce photocontrol effects but they are “damped” by radiation at other wavelengths and affected by greatly differing doses.

Therefore, the research in the effect of UV radiation required a narrow-band source that would allow wide variation in the irradiation dose. This concept was tested [46]. The research was conducted in the photocontrol effect of narrow-band UV radiation of DBD-driven KrBr and XeCl excilamps on accumulation of photosynthetic pigments in 50-day germs grown in laboratory conditions: Siberian cedar (*Pinus sibirica* Du Tour), Ajan spruce (*Picea ajanensis* Lindl. et Gord. (Fisch. ex Carr.)), and Cajander larch (*Larix cajanderi* Mayr (Worosch)). The research results showed that irrespective of the radiation wavelength, exposure time, and plant type, UV radiation stimulated the synthesis of chlorophyll. This suggests that narrow-band UV radiation displays photocontrol effects, which is of interest in terms of increasing the plant productivity, and that further research in UV excilamps can provide their use in photobiology of plants.

Another line of our studies concerns the application of excilamps for pre-sowing treatment of seeds. For tests, we chose a DBD-driven XeCl excilamp with an intense emission band at 290–320 nm corresponding to short-wave UV light transmitted through atmosphere. The irradiated materials were seeds of different varieties of flaxes, potatoes, carrots, and cucumbers. The radiation action on different varieties was found to be differential. However, in all cases, an increase was observed in germinating power, leaf coverage, and stem length, which increased the crop yield. The research results were patented [47].

The effects revealed put an interesting scientific question of what photochemical processes are responsible for them. We hope that an answer to this question will be found in the future.

6. Conclusions

Well-known DBD-driven excilamps operating on rare gases or mixtures of rare gases with halogens are effective sources of UV and VUV radiation. The design and some technical characteristics of DBD-driven excilamps and excilamp-based photochemical reactors developed in the IHCE RAS, Tomsk, Russia are presented. Besides that, the data about rather new types of excilamps excited by the runaway electrons preionized diffuse discharge both in single and pulse-periodic modes are given as well. High intensity emission radiation of homo- and hetero-nuclear dimers of rare gases, halides of rare gases molecules are obtained. The maximum power ~ 1 $MW \cdot cm^{-3}$ and the shortest radiation pulse width ~ 8 ns were registered in xenon at the pressure increasing up to 12 atm. It was shown, when during the breakdown of 0.5 mm gap by voltage pulses with an amplitude of ~10 kV and a repetition frequency of 1 kHz the main contribution to the plasma emission is made by the lines of electrode material and continuum radiation, about ~40 % of the total radiation energy being concentrated in the 200 – 300 nm range.

The rather new classes of scientific and industrial tasks of excilamps applications such as high-pressure gas-phase VUV photochemistry, physiological action of radiation on living organisms, effect of UV radiation on animals, plants and seeds are described.

Acknowledgment

The work is performed in the framework of the Russian Science Foundation, the project No. 14-29-00052.

Symbols used

d - interelectrode gap

Rg – rare gas atom

t^k - time interval during which the radiation flux of an excilamp decreases by k percent

X – halogen's atom

λ – wavelength

References

1. E. A. Sosnin, V. F. Tarasenko, M. I. Lomaev, *UV and VUV excilamps*. LAP LAMBERT Academic Publishing, Saarbrücken, Deutschland/Germany 2012. ISBN 978-3-695-21756-2.

2. B. Eliasson and U. Kogelschatz, *IEEE Trans. Plasma Sci.* 1991, *19 (6)*, 1063–1077.

3. U. Kogelschatz, *Plasma Chem. Plasma Process*. 2003, *23 (1)*, 1–46.

4. I. W. Boyd, J.-Y. Zhang, U. Kogelschatz, In *Book Photo-Excited processes, Diagnostics and Applications,* (Ed. A. Peled), Kluwer Academic Publishers, The Netherlands 2003, 161–199.

5. T. Oppenländer, *Photochemical Purification of Water and Air, Advanced Oxidation Processes (AOPs): Principles, Reaction Mechanisms, Reactor Concepts*, Wiley-VCH, New York/Weinheim 2003. ISBN 3-527-30563-7.

6. I. W. Boyd and I. I. Liaw, *Development and application of UV excimer lamps from 354nm -126 nm*. Proc. SPIE 6261(2006), High-Power Laser Ablation VI, 626104; doi:10.1117/12.686233.

7. I. I. Liaw and I. W. Boyd in *Functionalized Nanoscale Materials, Devices and Systems* (Eds: A. Vaseashta and I. N. Mihailescu), Springer 2008, 61–76.

8. U. Kogelschatz, *J. Opt. Technol.* 2012, 79 (8), 484-493.

9. T. Oppenländer, In *CRC Handbook of Organic Photochemistry and Photobiology*, 7th ed. (Eds. A. G. Griesbeck, M. Oelgemöller, F. Ghetti), CRC Press, Boca Raton 2012, 21–48.

10. K.-H. Pfoertner, and T. Oppenländer, *Photochemistry*. Ullmann's Encyclopedia of Industrial Chemistry, Published Online: 15 APR 2012. DOI: 10.1002/14356007.a19_573.pub2.

11. N. Christofi, M. A. Misakyan, G. G. Matafonova, E. M. Barkhudarov, V. B. Batoev., I. A. Kossyi, J. Sharp, *Chemosphere* 2008, 73, 717–722.

12. T. Oppenländer, G. Baum, *Wasser-Abwasser* 1996, *137 (6)*, 321–325.

13. G. G. Matafonova, N. Christofi, V. B. Batoev, E. A. Sosnin, *Chemosphere* 2008, 70, 1124-1127.

14. O. N. Tchaikovskaya, I. V. Sokolova, G. V. Mayer, E. A. Karetnikova, L. V. Nechaev, V. F. Tarasenko, E. A. Sosnin, *Atmos. Oceanic Opt.* 2010, *23 (1)*, 55-59.

15. M. Gomez, M.D. Murcia, N. Christofi, E. Gomez, J.L. Gomez, *Chem. Eng. J.* 2010, *158 (2)*, 120–128. DOI:10.1016/j.cej.2009.12.015

16. G. G. Matafonova, V. B. Batoev, *Water: chemistry and ecology* 2013, *9*, 87-92.

17. M. Buonanno, G. Randers-Pehrson, A. W. Bigelow, S. Trivedi, F. D. Lowy, H. M. Spotnitz, S. M. Hammer, D. J. Brenner, *PLoS ONE* 2013, *8(10)*, e76968. DOI:10.1371/journal.pone.0076968.

18. *Runaway Electrons Preionized Diffuse Discharges* (Ed. by V. F. Tarasenko), Nova Science Publishers, Inc., New York 2014.

19. *Excimer lasers* (Ed. by Ch. K. Rhodes), Springer-Verlag, Berlin Heidelberg, New York 1979.

20. A. N. Zaidel, E. Ya. Shraider, *Spectroscopy of vacuum ultraviolet*, Nauka, Moscow 1967.

21. A. M. Boichenko, A. V. Fedenev, in *Encyclopedia of Low Temperature Plasma, Series B, Reference appendices, databases, and databanks, V. XI-4. Gas and plasma lasers* (Ed by S. I. Yakovlenko), Fizmatlit, Moscow 2005, 546–568.

22. M. I. Lomaev, G. A. Mesyats, D. V. Rybka, V. F. Tarasenko, E. Kh. Baksht, *Quantum Electron.* 2007*, 37 (6)*, 595–596.

23. S. I. Yakovlenko, in *Encyclopedia of Low Temperature Plasma, Introductory volume IV.* (Ed. by V. E. Fortov), Nauka, MAIK Nauka/Interperiodica, Moscow 2000, 262–291.

24. E. Kh. Baksht, M. I. Lomaev, D. V. Rybka, V. F. Tarasenko, *Quantum Electron*. 2006, *36 (6)*, 576–580.

25. A. A. Ionin, A. V. Konyashchenko, B. M. Koval'chuk, O. N. Krokhin, V. F. Losev, G. A. Mesyats, L. D. Mikheev, A. G. Molchanov, Yu. N. Novoselov, L. V. Seleznev, D. V. Sinitsyn, A. N. Starodub, V. F. Tarasenko, S. I. Yakovlenko, V. D. Zvorykin, *Proc. of SPIE* 2007, 6735, 67350K1-10.

26. E. Kh. Baksht, A. M. Boichenko, I. V. Galakhov, V. I. Zolotovskii, M. I. Lomaev, V. A. Osin, D. V. Rybka, V. F. Tarasenko, A. N. Tkachev, and S. I. Yakovlenko, *Laser Phys.* 2007*, 17 (6)*, 782–797.

27. A. M. Boichenko, S. I. Yakovlenko, *Quantum Electron.* 2006, *36 (12)*, 1176–1180.

28. G. N. Zvereva, M. I. Lomaev, D. V. Rybka, V. F. Tarasenko, *Opt. Spectrosc.* 2007, *102 (1)*, 46–53.

29. G. N. Gerasimov, B. E. Krylov, M. I. Lomaev, D. V. Rybka, V. F. Tarasenko, *Quantum Electron.* 2010*, 40 (3)*, 241–245.

30. G. N. Gerasimov, *Usp. Fiz. Nauk* 2004, *174 (2)*, 155–175.

31. M. V. Erofeev, V. F. Tarasenko, *Quantum Electron.* 2008, *38 (4)*, 401–403.

32. M. I. Lomaev, D. V. Rybka, D. A. Sorokin, V. F. Tarasenko, K. Yu. Krivonogova, *Opt. Spectrosc.* 2009, *107,* 37–44.

33. E. Kh. Baksht, V.F. Tarasenko, Yu. V. Shut'ko, M. V. Erofeev, *Quantum Electron.* 2012, *42 (2)*, 153-156.

34. E. A. Sosnin, M. V. Erofeev, in *Proc. 3rd School-Workshop for Young Scientists of Russia*, BSC SB RAS, Ulan-Ude, 2004, 247−248 (in Russian).

35. Yu. V. Medvedev, V. G. Ivanov, N. I. Sereda, Yu. I. Polygalov, V. I. Erofeev, S. D. Korovin, M. V. Erofeev, E. A. Sosnin, A. I. Suslov, V. F. Tarasenko, V. A. Istomin, *Sci. Tech. Gas Industr*. 2004, *3*, 83–87. (in Russian).

36. M. G. Gonzalez, E. Oliveros, M. Wörner, A. M. Braun, *J. Photochem. Photobiol. C.* 2004, *5*, 225-246.

37. S. B. Alekseev, V. A. Kuvshinov, A. A. Lisenko, M. I. Lomaev, V. M. Orlovskii, V. A. Panarin, E. A Rozhdestvenskii, V. S. Skakun, V. F. Tarasenko, *Instrum. Exp. Tech.* 2006, *49 (1)*, 132–134.

38. A. Yu. Akhmedov, V. I. Erofeev, M. V. Erofeev, V. A. Istomin, S. D. Korovin, Yu. V. Medvedev, Yu. I. Polygalov, V. M. Orlovsky, O. A. Sergeev, E. A. Sosnin, V. P. Stepanov, V. F. Tarasenko, *Patent RU No. 2284850*, 2006.

39. J. A. Parrish and K. F. Jaencke, *J. Invest. Dermatol*. 1981, *76*, 359–362.

40. M. Mori, P. Campolmi, L. Mavilia, R. Rossi, P. Cappugi, N. Pimpinelli, *J. Am. Acad. Dermatol.* 2004, *50 (6)*, 943–945.

41. A. Ohtsuki, T. Hasegawa, E. Komiyama, A. Takagi, J. Kawasaki, S. Ikeda. *Indian J Dermatol.* 2013, *58*, 326. DOI:10.4103/0019-5154.113954.

42. E. A. Sosnin, I. I.Volotko, D. N. Saphonof, in *Proc. 11th Int. Conf. on Atomic and Molecular Pulsed Lasers*, Tomsk, 2013.

43. E. A. Sosnin, V. F. Tarasenko, I. I. Volotko, D. N. Safonov, *Patent RU No. 129761*, 2012.

44. M. Tosserams, J. Rozema, *Environ. Pollut.* 1995, *89*, 209–214.

45. E. A. Petrova, O. G. Bender, M. S. Yamburov, E. A. Sosnin, S. M. Avdeev, in *Proc. 3rd All-Russia Conf. of Young Scientists*, IAO SB RAS, Tomsk, 2006, 470-473. (in Russian).

46. O. G. Bender, E. A. Petrova., A. P. Zotikova, E. A. Sosnin, S. M. Avdeev, *Vestnik TSU*, 2006, *67 (2)*, 15-24. (in Russian).

47. E. A. Sosnin, V. F. Tarasenko, V. A. Panarin, Yu. V. Chudinova, I. A. Viktorova, A. E. Cheglokov, *Patent RU No. 139005*, 2013.

Figure legends

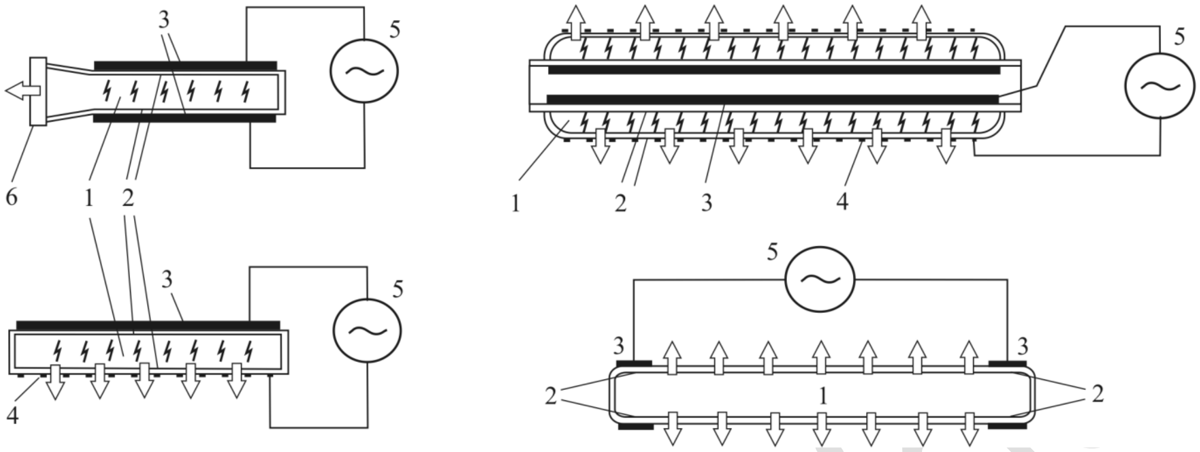

Figure 1. Designs of DBD-driven excilamps: 1- gas gap, 2 – quartz wall, 3, 4 – electrodes, 5 – power supply, 6 – output window.

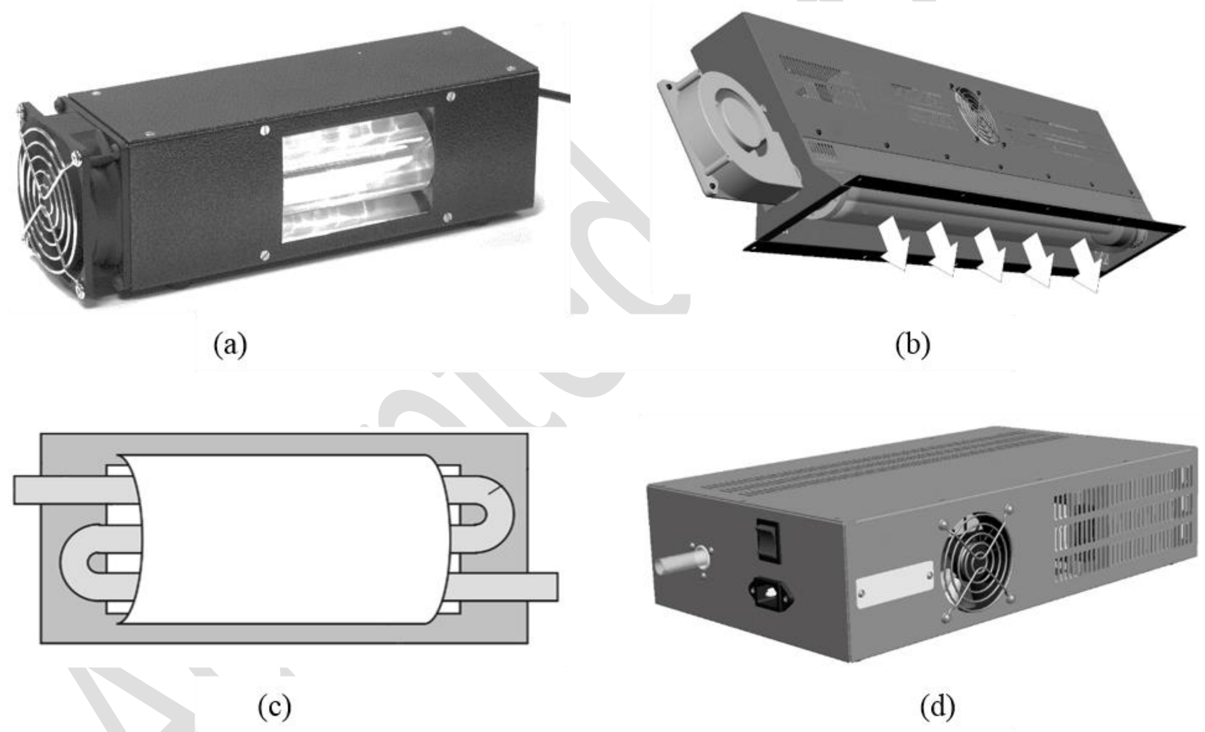

Figure 2. Design of a DBD-driven excilamps (a, b) and photoreactors based on a DBD-driven excilamps (c, d).

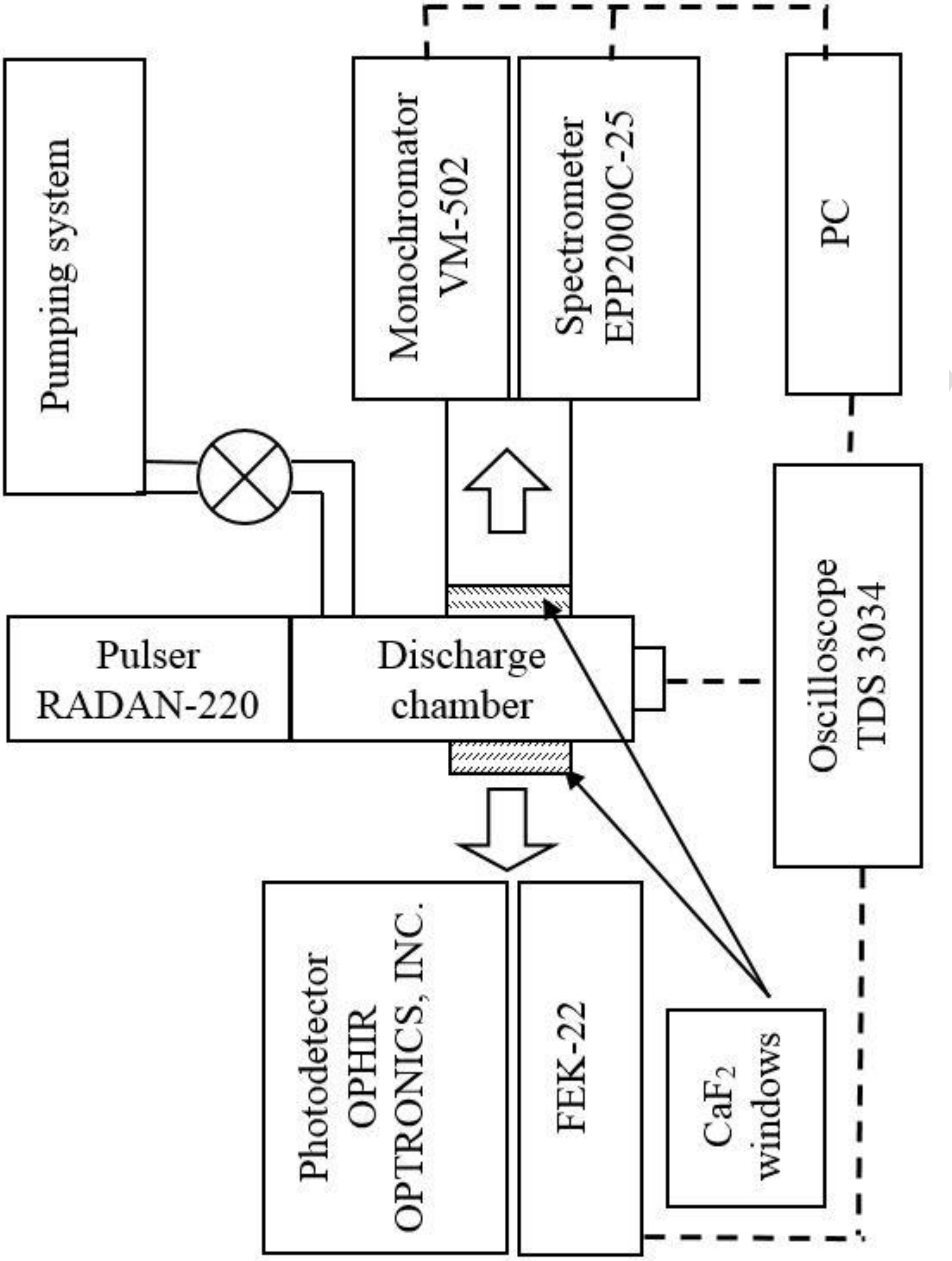

Figure 3. Block diagram of experimental setup.

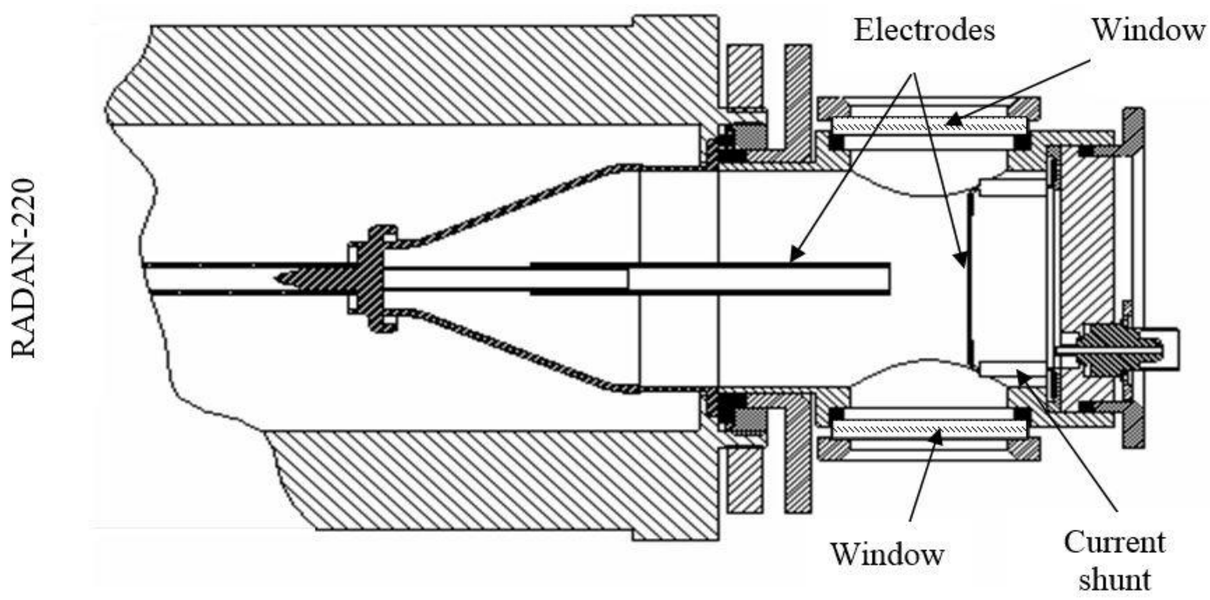

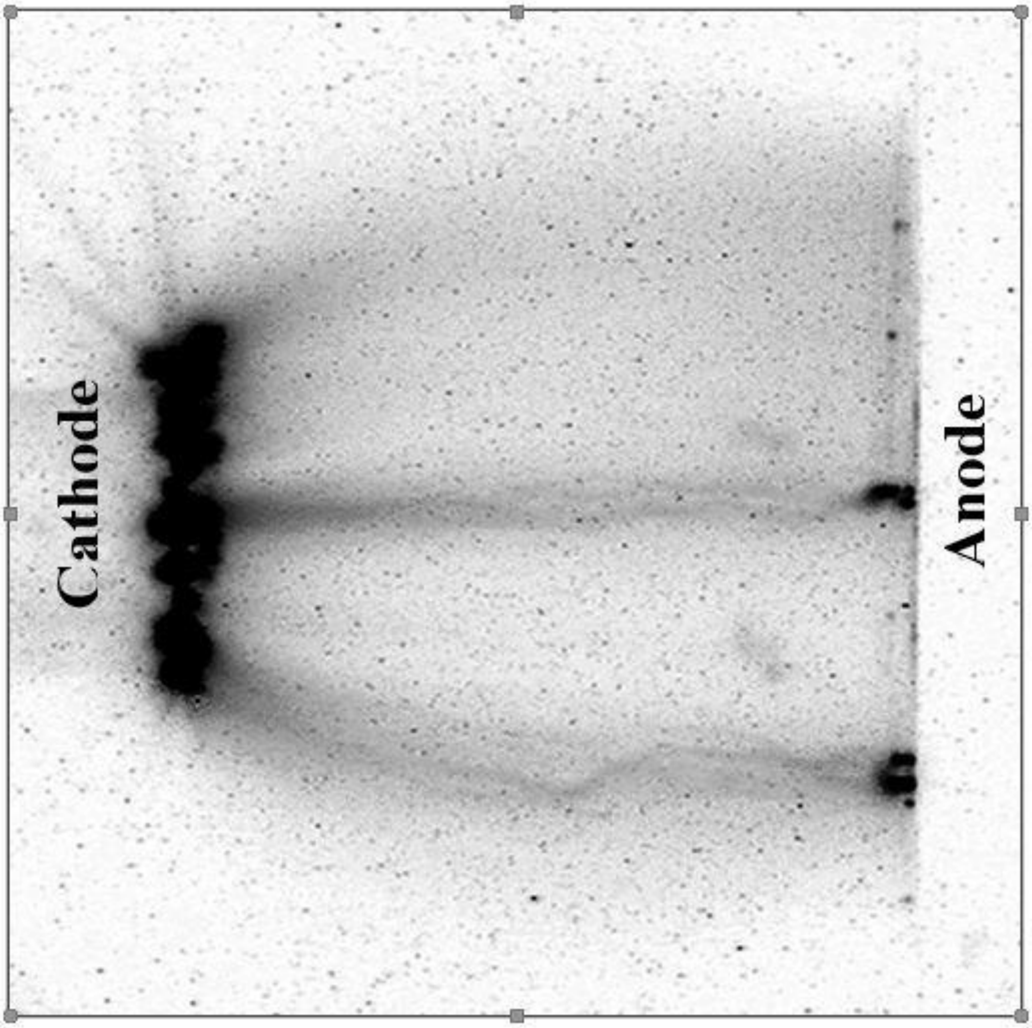

Figure 4. The design of gas diode (a); appearance of the discharge glow in xenon at a pressure of 1.2 atm (b).

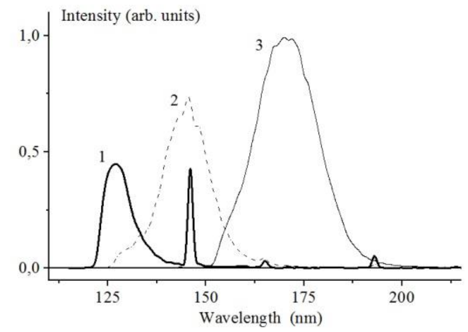

Figure 5. Broadband radiation spectra of argon with admixture of xenon (less than 0.01%) (1), krypton (2) and xenon (3) dimers at pressure of 1.2 atm.

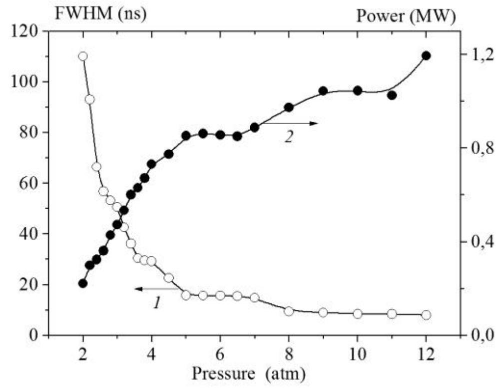

Figure 6. Full width at half maximum (FWHM) (1) and maximal pulse power of xenon dimer radiation on xenon pressure.

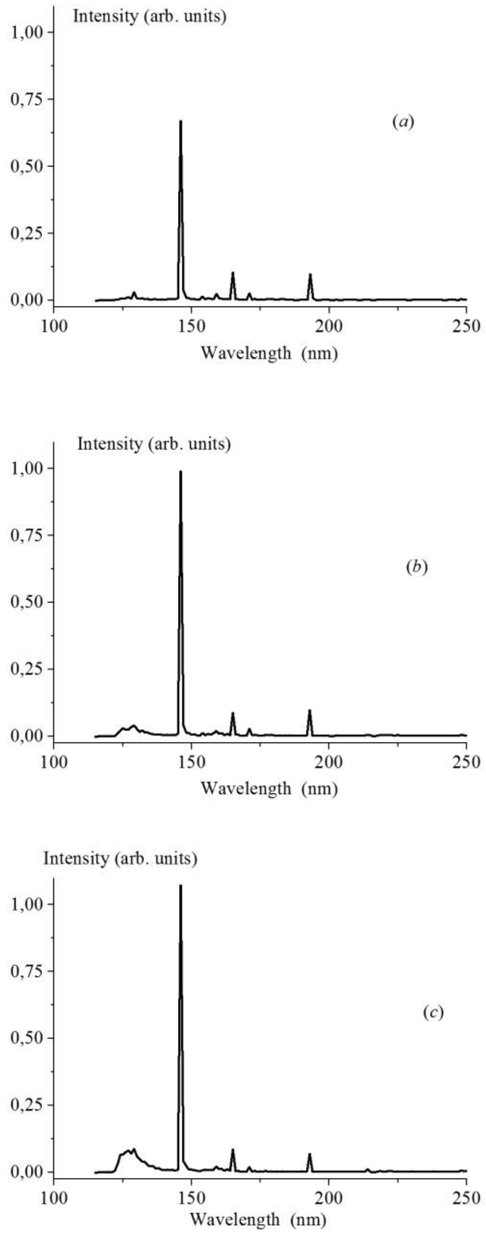

Figure 7. Emission spectra of REP DD in argon with xenon admixture (~0.01%) at pressure of 0.3 (a), 0.6 (b), 0.9 (c) and 1.2 (d) atm.

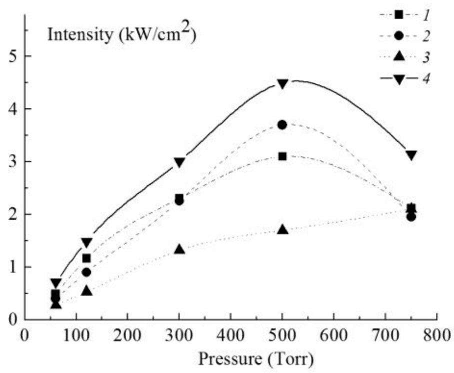

Figure 8. Pulsed intensity of emission radiation on the $XeCl^*$ (*1*), $KrCl^*$ (*2*), $KrBr^*$ (*3*) and $XeBr^*$ (*4*) molecules transitions on the pressure of working gas mixture. Gas mixture composition: Xe/Cl_2, Kr/Cl_2, Xe/Br_2=50/1; Kr/Br_2=100/1.

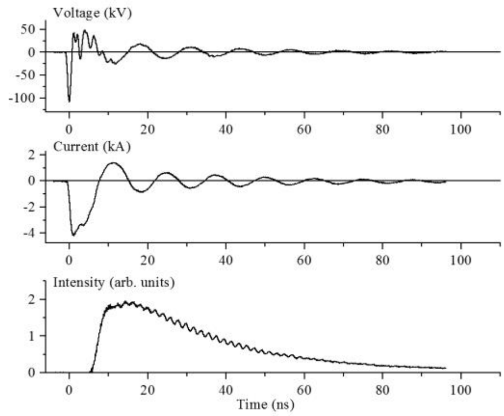

Figure 9. Waveforms of voltage, discharge current and emission radiation pulses of REP DD in Xe/Br_2=50/1 gas mixture at pressure of 500 Torr.

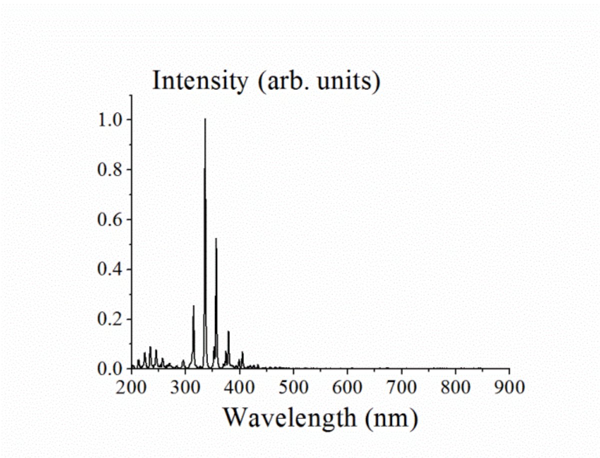

Figure 10. The spectrum of REP DD plasma in atmospheric-pressure nitrogen. Single mode.

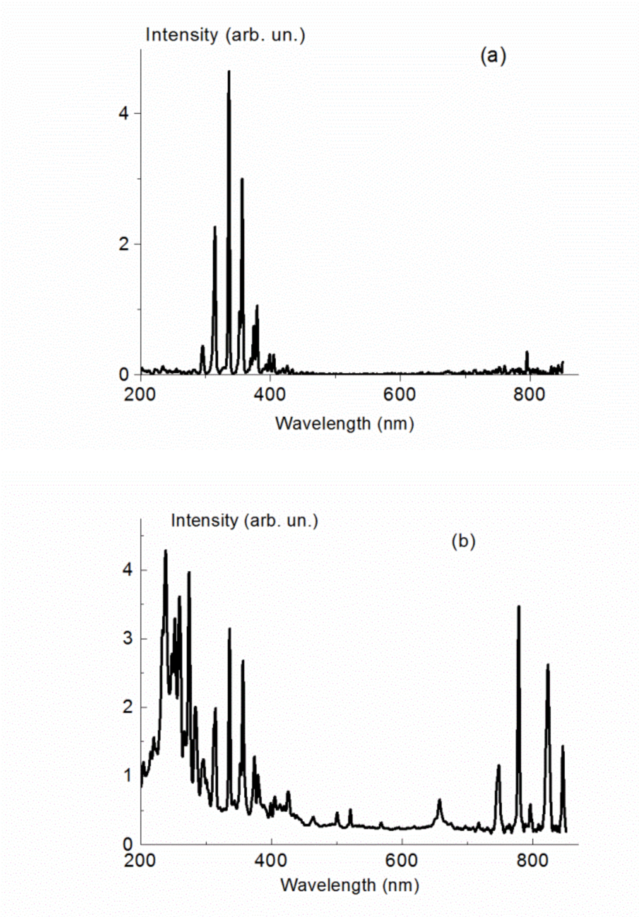

Figure 11. Emission spectra of REP DD radiation in nitrogen (a) and at transition of REP DD in air to spark (b). The nitrogen and air pressure is 1 atm; in both cases stainless steel electrodes were used. Pulse repetition rate is 60 Hz.

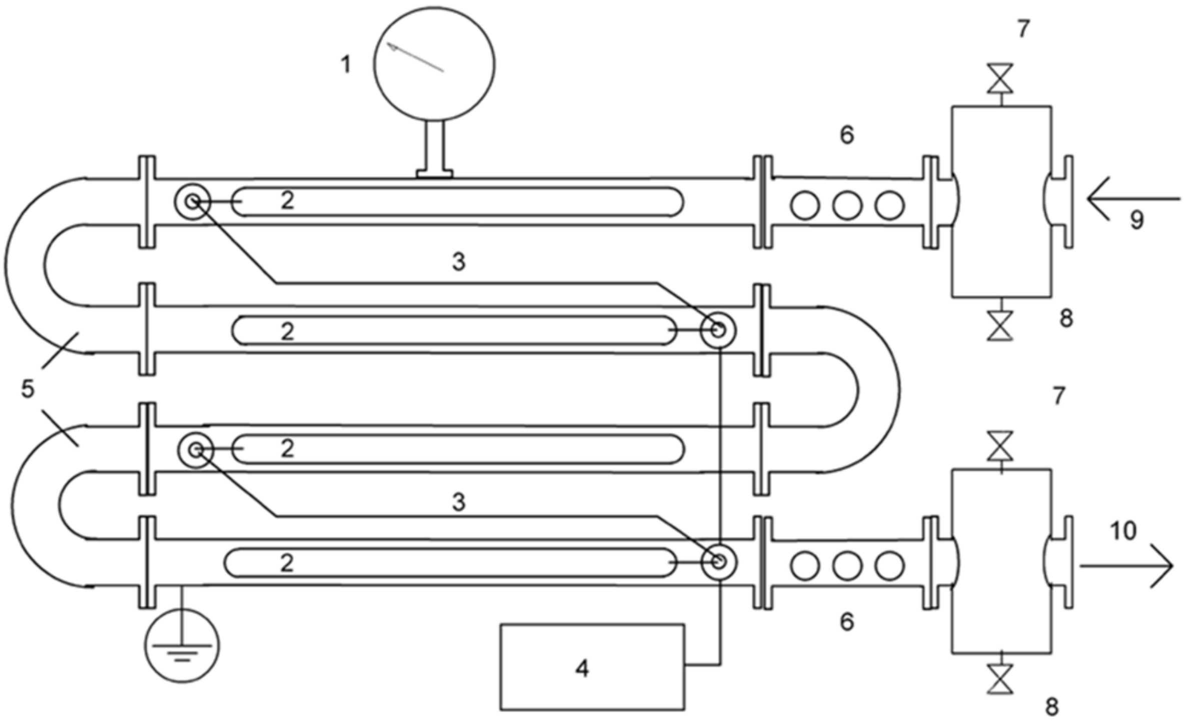

Figure 12. Setup for pilot research in natural gas conversion: 1 – pressure gauge; 2 – excilamps on xenon dimers; 3 – high-voltage leads; 4 – excilamp power supply; 5 – main; 6 – sensors of gas moisture, temperature, and flow rate; 7 – gas extraction; 8 – gas condensate extraction; 9 – gas supply from a gas pipeline; 10 – exhaust.

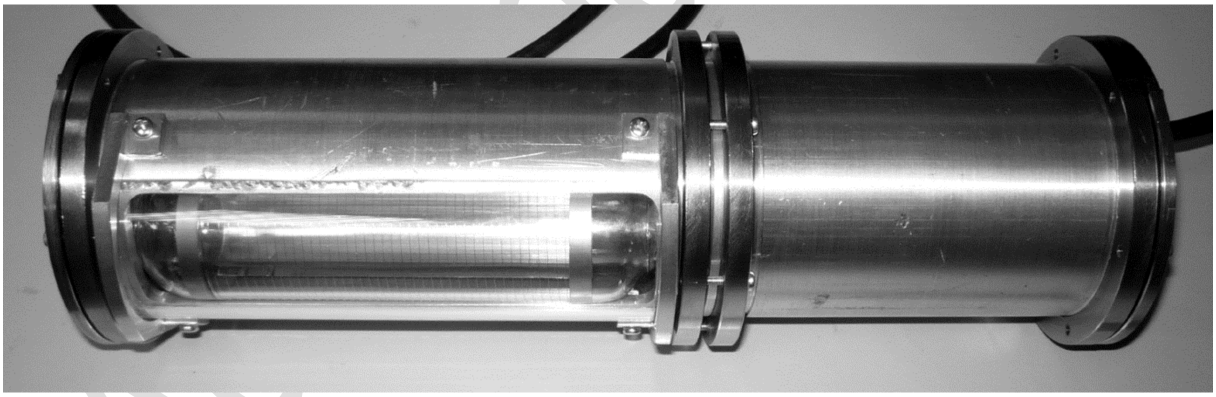

Figure 13. Appearance of the protected XeCl excilamps with no cooling.

Tables with headings

Table 1.

Rare gas (*Rg*)			Ar	Kr	Xe
Halogen (X_2)			126 nm	146 nm	172 nm
	Cl	259 nm	175 nm	222 nm	308 nm
	Br	289 nm	165 nm	207 nm	282 nm

Table 1. Most-used maximum radiation wavelengths for excimer (X_2^*, Rg_2^*) and exciplex (RgX^*) molecules in rare gases *Rg*, halogens *X*, and their mixtures Rg-X_2.

Table 2.

Working molecule	Peak wavelength, nm	Window dimensions, mm	Power consumption, W	Radiant exitance, mW/cm^2
XeCl	308	60 × 90	40	18
KrBr	206	60 × 90	40	9
KrCl	222	60 × 100	30	10
XeBr	282	60 × 90	35	20
Br_2*	291.6	60 × 100	35	4
I_2*	342	60 × 100	35	1.5
Cl_2*	257.8	60 × 100	35	2
Xe_2*	172	60 × 100	35	30

Table 2. Parameters of BD_P (barrier discharge, portable) excilamps.

Table 3.

Working molecule	XeCl*, KrBr*, KrCl*, XeBr*
Peak wavelength, nm	308, 207, 222, 283
Hosing dimensions, mm	250 × 100 × 420
Tube dimensions, mm	Ø 14 × 480
Power consumption, W	≤ 150
Irradiated zone length, mm	300

Table 3. Parameters of BD_R (barrier discharge, reactors) photoreactors.

Table 4.

ELEMENT	ELEMENTAL COMPOSITION OF NATURAL GAS, MASS %		
	nonirradiated	Xe_2 excilamp	KrCl excilamp
Methane	82.85	82.91	81.92
Carbon dioxide	0.98	0.98	1.02
Ethane	5.85	5.85	6.10
Water	0.25	0.15	0.19
Propane	5.17	5.00	5.39
i-Butane	1.83	1.81	1.90
n-Butane	1.71	1.69	1.83
i-Pentane	0.67	0.66	0.76
n-Pentane	0.46	0.45	0.48
C_{6+}	0.23	0.50	0.40

Table 4. Elemental composition of natural gas before and after VUV (Xe_2 excilamp) and UV (KrCl excilamps) irradiation [35].

Table of Contents: Graphical Abstracts

Excilamps are effective sources of spontaneous narrowband radiation in the UV or VUV spectral regions. They operate due to formation and subsequent decay of excimer or exciplex molecules. Long lifetime (up to 10000 h) and possibility of change of radiation wavelength with choice of working excimer/exciplex molecule are attractive features of photoreactors based on excilamps

.